Mechanism of Bubble Formation in the Drying of Polymer Films

Reza Pourdarvish, Ronald P. Danner, J. Larry Duda

Department of Chemical Engineering, Center for the Study of Polymeric Systems, The Pennsylvania State University, University Park, Pennsylvania 16802

Received 29 February 2008; accepted 23 July 2008
DOI 10.1002/app.28998
Published online 3 October 2008 in Wiley InterScience (www.interscience.wiley.com).

ABSTRACT: A common problem in making thin polymer films by solution processing is the undesirable formation of bubbles during the drying process. These bubbles appear well below the boiling point of the solvent. Experience indicates, however, that the degassing of the polymer solutions reduces bubble formation, indicating a relationship with the presence of air. This work is based on a hypothesis that if the solubility of air in the polymer solution increases with solvent concentration, then the solution can become supersaturated with air as the concentration of the solvent is reduced during the drying process. To test this hypothesis the system poly(vinyl acetate)-toluene-nitrogen was chosen. Previously published data on the solubility and diffusion of nitrogen in the polymer-solvent system were used. Different diffusion models based on the friction coefficients and free-volume model were then used to correlate the diffusivity data so that the diffusion behavior of the ternary system can be predicted over a broad range of conditions. Finally, the thermodynamic and diffusivity correlations were incorporated into a multicomponent drying model which included main and cross-diffusion terms to predict saturation behavior in the polymer solution during the drying process. The model without the cross-diffusion terms represents the ideal system in which the diffusion of one component does not affect the diffusion of others. The drying model did not predict supersaturation of nitrogen when cross-diffusion terms were neglected. Supersaturation of nitrogen was predicted, however, when the cross-diffusion terms are included. Therefore, the cross-diffusion terms in the mass transfer model are essential for the development of nitrogen supersaturation. Also different diffusion models based on the friction coefficients led to qualitatively similar predictions for the supersaturation of nitrogen. The simulation's results supported our experimental observations regarding bubble formation. J Appl Polym Sci 111: 417–428, 2009

Key words: coatings; diffusion; phase separation; processing; thermodynamics

INTRODUCTION

In the drying of a polymer solution in a convective oven, bubbles can be created in the film. The vapor pressure of the volatile solvent is one of the reasons for bubble nucleation in the polymer-solvent mixture. But during drying, bubbles can also develop and grow well below the boiling point of the solvent in the film. This indicates another mechanism exists for bubble formation.

This project was initiated on the premise that the supersaturation of air (oxygen and nitrogen) in a polymer solution during drying can lead to bubble or blister defects in the resulting coating. Observation supports the original premise that degassing polymer solutions before drying can reduce bubble formation. The system of poly(vinyl acetate), toluene, and nitrogen was used to evaluate this potential source of coating defects.

Correspondence to: R. P. Danner (rpd@psu.edu).

Journal of Applied Polymer Science, Vol. 111, 417–428 (2009)

If the solubility of nitrogen increases with the concentration of toluene in the polymer solution, then there is the potential for supersaturation of nitrogen as the toluene concentration decreases during the drying process. In this mechanistic point of view the assumption is that before and during the drying process, the polymer solution has exposure to a vapor environment in which the activity of nitrogen is constant. Figure 1 shows the saturation line which represents the equilibrium concentration of air and solvent in the polymer-solvent mixture. The air or nitrogen concentration is initially high, Point 1. As solvent is removed the solution can become supersaturated in air (Point 3). This suggests that bubble formation would likely occur if there is a nucleation site such as an impurity or cavity.

METHODOLOGY

To model the drying, knowledge of the vapor-liquid equilibria of the binary and ternary mixtures is necessary. In a previous publication[1] solubility and diffusion data for the relevant systems were obtained

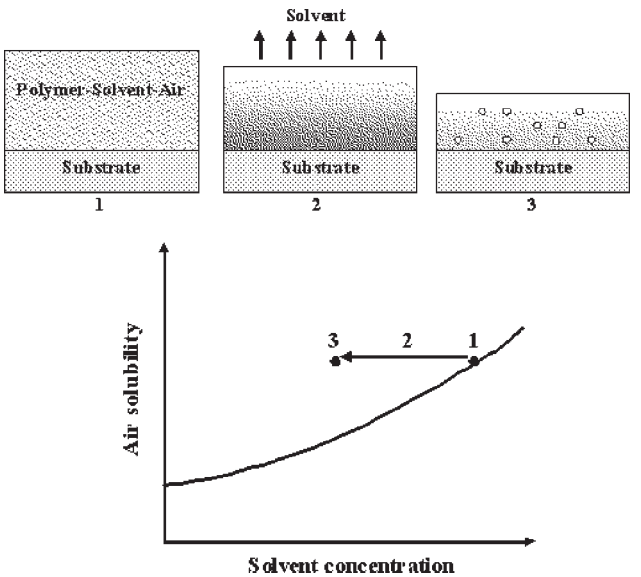

Figure 1 Mechanism of bubble formation during drying process due to air supersaturation.

by the pressure decay method over ranges of temperature and concentration. The solubility data were correlated using the group-contribution, lattice-fluid equation of state (GCLF-EoS).[2] The saturation line and thermodynamics (chemical potentials) of the polymer solution were then predicted using this equation of state. Self-diffusion coefficients were correlated using the free-volume theory of Vrentas and Duda.[3,4] Mutual-diffusion coefficients, which are a function of chemical potentials and self-diffusion coefficients, were then estimated from several models which use different friction coefficient ratios. This procedure is shown schematically in Figure 2.

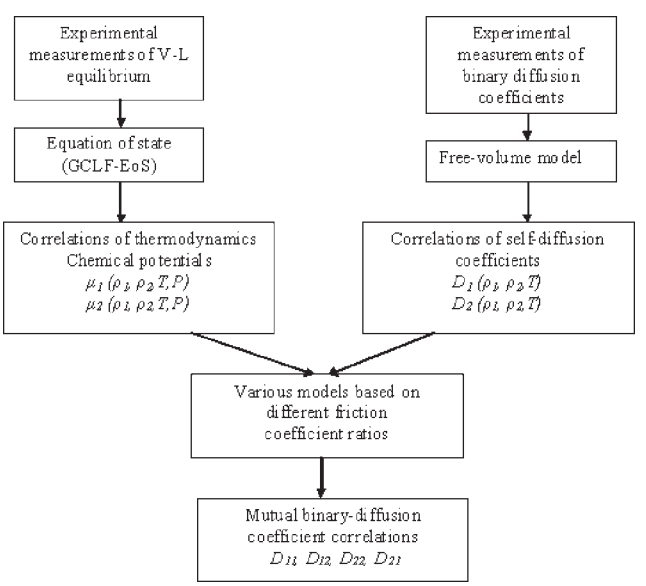

Figure 2 Procedure for calculation of the main and cross mutual-diffusion coefficients.

A drying model was developed to predict the concentration of toluene and nitrogen as a function of time and position during the drying operations. Of particular interest was the comparison of nitrogen concentrations in the solution with the nitrogen solubility at any time and position in the film. If the predicted nitrogen concentration goes above the nitrogen saturation line, the potential for bubble formation due to nitrogen supersaturation exists. Consequently, the drying process can be designed to eliminate or minimize nitrogen supersaturation.

Figure 3 shows the procedure to predict the concentrations in the coated film at any position and time using the thermodynamics of the solution, the mutual-diffusion coefficients, the thermal properties of components, and the process conditions. Comparison between the concentrations of nitrogen in the solution as it dries and its saturation value will indicate whether nitrogen becomes supersaturated or not.

BENCH EXPERIMENT OBSERVATIONS

During the drying of a coated polymer-solvent solution [poly(vinyl acetate) and toluene] on the bench, the following were observed.

1. Bubbles were created well below the boiling point of the solvent.
2. Bubble formation was increased when the flow rate of air increased in the convective oven, thus increasing the mass transfer in the gas phase.
3. Degassing the solution before drying reduced bubble formation.
4. Bubble formation was increased by increasing the oven temperature

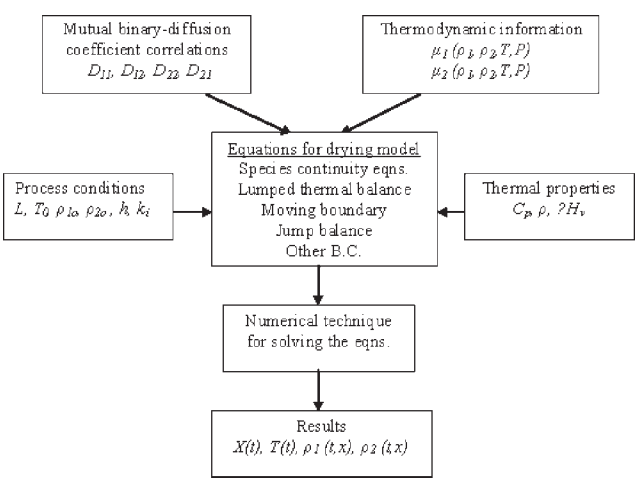

Figure 3 Procedure for calculation of concentration of nitrogen and toluene during the drying of a polymer solution.

TABLE I
The Free-Volume Parameters for Toluene and Poly(vinyl acetate) Reported by Different Researchers

Parameter	Zielenski and Duda[6]	Vrentas et al.[7]
$D_{01} \times 10^4$ (cm^2/s)	4.82	82.5
$\frac{K_{11}}{\gamma} \times 10^3$ [cm^3/(gK)]	1.4	1.57
$\frac{K_{13}}{\gamma} \times 10^4$ [cm^3/(gK)]	4.33	4.33
$K_{21} - T_{g1}$ (K)	−86.32	−90.5
$K_{23} - T_{g3}$ (K)	−258.2	−256
$\hat{V}_1^*$ (cm^3/g)	0.917	0.917
$\hat{V}_3^*$ (cm^3/g)	0.728	0.728
ξ_{13}	0.82	0.77
E (cal/mol)	0.0	1,860

Indices 1 and 3 refer to toluene and poly(vinyl acetate), respectively.

SELF-DIFFUSION COEFFICIENTS

Vrentas et al.[5] developed a model for the self-diffusion coefficients in a ternary system comprised of two solvents and a polymer using the free-volume theory.

$$D_1 = D_{01} \exp\left(\frac{-E}{RT}\right) \times \exp\left(\frac{-\gamma(\omega_1 \hat{V}_1^* + \omega_2 \hat{V}_2^* \frac{\zeta_{13}}{\zeta_{23}} + \omega_3 \hat{V}_3^* \zeta_{13})}{\hat{V}_{FH}}\right) \quad (1)$$

$$D_2 = D_{02} \exp\left(\frac{-E}{RT}\right) \times \exp\left(\frac{-\gamma(\omega_1 \hat{V}_1^* \frac{\zeta_{23}}{\zeta_{13}} + \omega_2 \hat{V}_2^* + \omega_3 \hat{V}_3^* \zeta_{23})}{\hat{V}_{FH}}\right) \quad (2)$$

$$D_3 = D_{03} \exp\left(\frac{-E}{RT}\right) \exp\left(\frac{-\gamma(\frac{\omega_1 \hat{V}_1^*}{\zeta_{13}} + \frac{\omega_2 \hat{V}_2^*}{\zeta_{23}} + \omega_3 \hat{V}_3^*)}{\hat{V}_{FH}}\right) \quad (3)$$

where,

$$\hat{V}_{FH} = \omega_1 K_{11}(K_{21} + T - T_{g_1}) + \omega_2 K_{12}(K_{22} + T - T_{g_2}) + \omega_3 K_{13}(K_{23} + T - T_{g_3}) \quad (4)$$

The parameters for each component can be obtained from viscosity and diffusivity data for binary solvent-polymer systems. Indices 1, 2, and 3 refer to toluene, nitrogen and poly(vinyl acetate), respectively. Several researchers have reported the free-volume parameters for poly(vinyl acetate) and toluene (Table I).

In the binary system of nitrogen and poly(vinyl acetate), the weight fraction (solubility) of nitrogen in the polymer is very small, and, therefore, the mutual diffusion and self-diffusion coefficients can be assumed to be equal. The free-volume parameters for nitrogen and poly(vinyl acetate) can be obtained using experimental diffusivity data at two different temperatures. Because of the low solubility of nitrogen, the weight fraction of nitrogen is assumed to be zero. Thus, considering E to be zero, eq. (2) determines D_{02} and ξ_{23}. By applying the free-volume parameters for poly(vinyl acetate) from Table I and diffusivity data from Pourdarvish et al.,[1] these two parameters are calculated as:

$$\xi_{23} = \frac{\ln \frac{D_{2,T_1}}{D_{2,T_2}}}{\frac{\hat{V}_3^*}{K_{23}} \left(\frac{-1}{(K_{33} + T_1 - T_{g_3})} + \frac{1}{(K_{33} + T_2 - T_{g_3})} \right)} \quad (5)$$

$$D_{02} = \frac{D_2}{\exp\left(\frac{-\gamma(\hat{V}_3^* \xi_{23})}{K_{23}(K_{33} + T - T_{g_3})}\right)} \quad (6)$$

where, D_{2,T_1} and D_{2,T_2} are the diffusion coefficients at different temperatures. As a check on the experimental data, the parameter ξ_{23} was also estimated from the Sugden group-contribution method.[8] The free-volume parameters of nitrogen in poly(vinyl acetate) are listed in Table II using experimental data and the Sugden estimation method. The agreement is quite good.

MUTUAL-DIFFUSION COEFFICIENTS

Intermolecular frictional forces have an important role in mutual diffusion in a polymer solvent solu-

TABLE II
The Two Free-Volume Parameters of Nitrogen in PVAc Using Binary Experimental Data at Different Temperatures

Parameter	Using PVAc free-volume parameters from Zielinski and Duda[6]	Using PVAc free-volume parameters from Vrentas et al.[7]	Sugden Estimation[8]
D_{02}	1.5×10^{-5}	1.7×10^{-5}	–
ξ_{23}	0.215	0.229	0.216

The parameters are compared with the Sugden group contribution method.

TABLE III
Ternary Mutual-Diffusion Parameters for Different Models

Model	A_{11}	B_{11}	A_{22}	B_{22}
Vrentas et al.[7]	$\frac{\rho_1 D_1 M_1}{RT}$	0	0	$\frac{\rho_2 D_2 M_2}{RT}$
Alsoy and Duda[13]	$\frac{\rho_1 D_1 M_1}{RT}[1-\rho_1\hat{V}_1]$	$-\frac{\rho_1\rho_2 D_2 M_2}{RT}[\hat{V}_2]$	$-\frac{\rho_1\rho_2 D_1 M_1}{RT}[\hat{V}_1]$	$\frac{\rho_2 D_2 M_2}{RT}[1-\rho_2\hat{V}_2]$
Zielinski and Hanley[14]	$\frac{\rho_1 D_1 M_1}{RT}[1-\rho_1\hat{V}_1+\rho_1\hat{V}_3]$	$\frac{\rho_1\rho_2 D_2 M_2}{RT}[\hat{V}_3-\hat{V}_2]$	$\frac{\rho_1\rho_2 D_1 M_1}{RT}[\hat{V}_3-\hat{V}_1]$	$\frac{\rho_2 D_2 M_2}{RT}[1-\rho_2\hat{V}_2+\rho_2\hat{V}_3]$
Price and Hadj Romdhane[15]	$\frac{\rho_1 D_1 M_1}{RT}\times\left[1-\rho_1\hat{V}_1\left(1-\frac{D_3\hat{V}_3M_3}{D_1\hat{V}_1M_1}\right)\right]$	$\frac{\rho_1\rho_2\hat{V}_2 D_2 M_2}{RT}\times\left(1-\frac{D_3\hat{V}_3M_3}{D_2\hat{V}_2M_2}\right)$	$\frac{\rho_2\rho_1\hat{V}_1 D_1 M_1}{RT}\times\left(1-\frac{D_3\hat{V}_3M_3}{D_1\hat{V}_1M_1}\right)$	$\frac{\rho_2 D_2 M_2}{RT}\times\left[1-\rho_2\hat{V}_2\left(1-\frac{D_3\hat{V}_3M_3}{D_2\hat{V}_2M_2}\right)\right]$

tion. Bearman's[9] statistical mechanical theory of diffusion shows that shortly after a system establishes a concentration gradient, a quasi-stationary regime is reached, in which the chemical potential gradient (driving force for diffusion) is equal to the frictional force in a multicomponent system. The frictional force in a multicomponent system is the sum of the individual forces between molecules in the system.[9]

$$\nabla\mu_i = -\sum_{j=1}^{n}\frac{\rho_j\zeta_{ij}(v_i-v_j)}{M_j} \tag{7}$$

According to Onsager,[10,11] the flux of a solute molecule is expressed by the concentration gradients of all the solutes. Thus, Cussler[12] introduced the following equation for ternary systems:

$$j_1^{\neq} = -D_{11}\nabla\rho_1 - D_{12}\nabla\rho_2 \tag{8}$$

$$j_2^{\neq} = -D_{21}\nabla\rho_1 - D_{22}\nabla\rho_2 \tag{9}$$

where D_{12} and D_{21} are the cross-diffusion coefficients, and D_{11} and D_{22} are the main diffusion coefficients. Four different models have been presented in the literature using different reference frame velocities to eliminate the friction coefficients: Vrentas et al.,[7] Alsoy and Duda,[13] Zielinski and Hanley[14] and Price and Hadj Romdhane.[15] The equations for the mutual-diffusion coefficients for a solvent-solvent-polymer system take the following forms, assuming that the polymer does not diffuse.[14]

$$D_{11} = A_{11}\left(\frac{\partial\mu_1}{\partial\rho_1}\right) + B_{11}\left(\frac{\partial\mu_2}{\partial\rho_1}\right) \tag{10}$$

$$D_{12} = A_{12}\left(\frac{\partial\mu_1}{\partial\rho_2}\right) + B_{12}\left(\frac{\partial\mu_2}{\partial\rho_2}\right) \tag{11}$$

$$D_{21} = A_{21}\left(\frac{\partial\mu_1}{\partial\rho_1}\right) + B_{21}\left(\frac{\partial\mu_2}{\partial\rho_1}\right) \tag{12}$$

$$D_{22} = A_{22}\left(\frac{\partial\mu_1}{\partial\rho_2}\right) + B_{22}\left(\frac{\partial\mu_2}{\partial\rho_2}\right) \tag{13}$$

where:

$$\begin{aligned} A_{11} &= A_{12} \qquad A_{22} = A_{21} \\ B_{11} &= B_{12} \qquad B_{22} = B_{21} \end{aligned} \tag{14}$$

Here, parameters A_{ij} and B_{ij} are defined for each model in Table III.

Figures 4 and 5 show the comparison between experimental data and the theoretical predictions of mutual-diffusion coefficients for the system of toluene-poly(vinyl acetate) at 60 and 90°C. In these graphs, the four different models were applied and the chemical potential gradients were calculated from the correlated GCLF-EoS.[2] The free-volume parameters were employed from Tables I and II. With the exception of the model presented by Vrentas et al., all the models predict a close fit to the

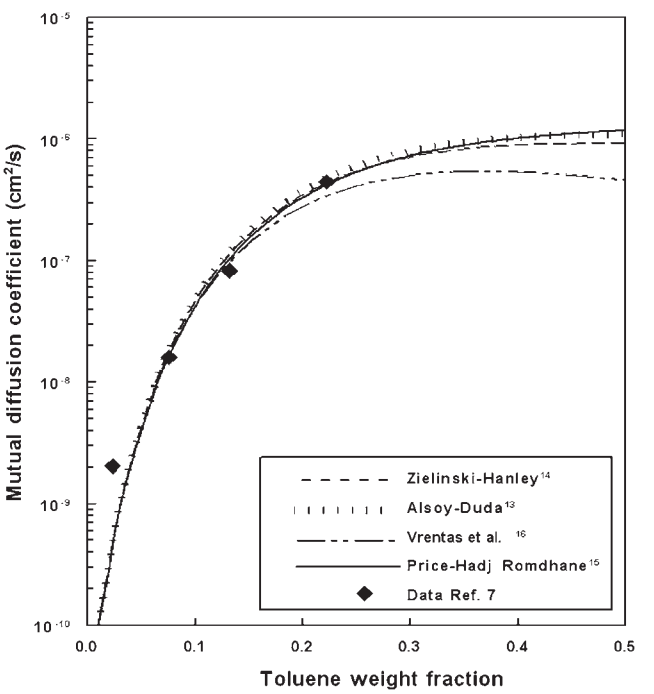

Figure 4 Experimental data[7] and the theoretical prediction for toluene/poly(vinyl acetate) mutual-diffusion coefficients at 60°C.

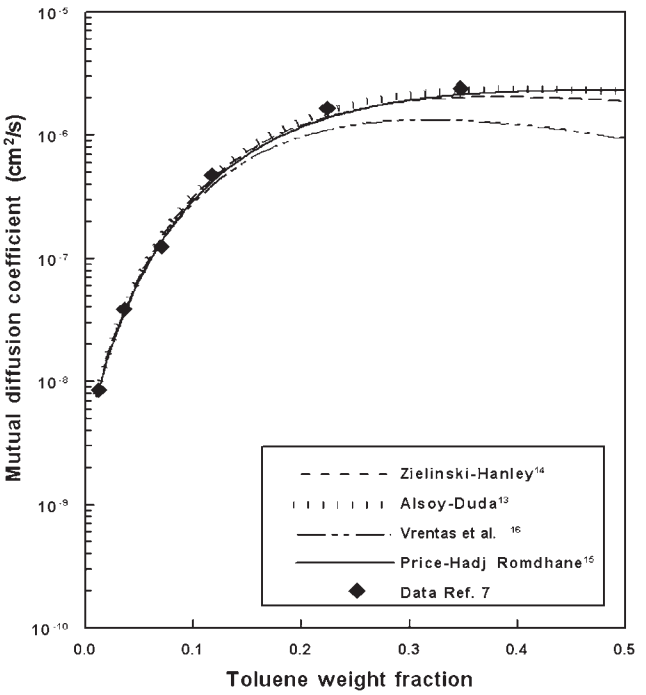

Figure 5 Experimental data[7] and the theoretical prediction for toluene/poly(vinyl acetate) mutual-diffusion coefficients at 90°C.

mutual-diffusion coefficients. The graphs indicate that the thermodynamics of the solution predict the behavior of the mixture well. The deviation of the Vrentas et al. model probably results from their assumption that the concentration of solvent was sufficiently small. As shown in these figures, when the concentration of solvent is small (less than 10 wt %), all models predict similar behavior.

Results show that in general the models are quite similar and that they show good agreement with the experimental data. This indicates that the thermodynamics of the system have been adequately treated.

DRYING MODEL

The drying of polymer-solvent coatings plays a major role in the manufacture of many products such as adhesives, tapes, paints, and photographic materials, etc. The overall process is similar for a variety of polymeric products. First, a solvent dissolves the polymer to make a solution. The solution is coated on an appropriate moving substrate, such as a conveyer belt which can be a polymer itself, or even a metal sheet. This coated film proceeds to an oven in which the solvent diffuses out of the film by direct contact with forced air convection. The drying involves simultaneous mass, heat, and momentum transfer in the polymeric solutions.

The general picture of drying geometry appears in Figure 6. The polymer film is uniformly coated on the substrate. The initial thickness of the polymer solution and substrate are L and H, respectively. The temperature of the gas phase on top of the polymer solution is T^G, and the heat transfer coefficient is h^G. The temperature and heat transfer coefficient in the gas phase below the substrate are T^g and h^g, respectively. The following lists the assumptions used to derive the model for the drying process.[13,17]

1. There is no significant solvent gradient or velocity in the y or z directions due to the small thickness of the film.
2. The specific partial volumes of solvents and polymer are independent of concentration (no volume change on mixing).
3. Axial diffusion and axial conduction are negligible.
4. Average values were used for the densities, heat capacities, and thermal conductivities of polymer and substrate.
5. The total mass density is a function of composition.
6. Viscous dissipation is negligible in the polymer film.
7. There is no radiative heat transfer.
8. There exists a single uniform temperature for the polymer film and substrate, i.e., the convective heat resistance is assumed to be much greater than the conductive resistance.

The equation for species continuity using volume-average velocity as a reference frame can be written, as:

$$\frac{\partial \rho_i}{\partial t} = \frac{\partial}{\partial x}\left(\sum_{j=1}^{n-1} D_{ij}\frac{\partial \rho_j}{\partial x}\right) \tag{15}$$

where D_{ij} are the main and cross mutual-diffusion coefficients in the polymer phase. The advantage of using the volume-average velocity instead of the mass-average velocity is that there is no convective term in the continuity equation. The boundary conditions at the interface of polymer and substrate are obtained using the jump balance for solvents.

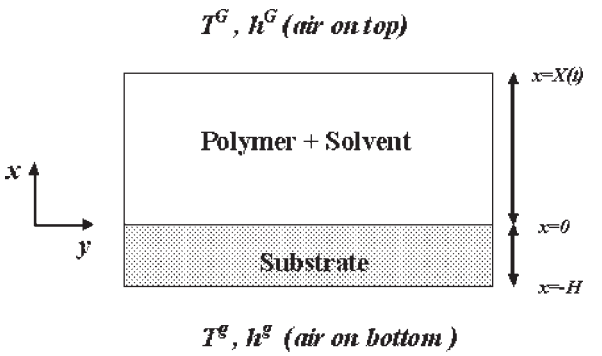

Figure 6 Schematic of film geometry in drying process.

TABLE IV
Drying Model in Dimensionless Form for Multicomponent Systems

Dimensionless variables

$$\bar{\rho}_i = \frac{\rho_i}{\rho_{i0}} \qquad \bar{X} = \frac{X}{L} \qquad \bar{t} = \frac{D_{11,0}t}{L^2} \qquad \bar{T} = \frac{T - T_0}{T^G - T_0}$$

Species continuity

$$\frac{\partial \bar{\rho}_i}{\partial \bar{t}} - \frac{\eta}{\bar{X}}\frac{d\bar{X}}{d\bar{t}}\frac{\partial \bar{\rho}_i}{\partial \eta} = \frac{1}{\bar{X}^2}\frac{\partial}{\partial \eta}\left(\sum_{j=1}^{n-1}\frac{D_{ij}}{D_{11,0}}\frac{\rho_{j0}}{\rho_{i0}}\frac{\partial \bar{\rho}_j}{\partial \eta}\right)$$

Boundary conditions

$$\frac{\partial \bar{\rho}_i}{\partial \eta} = 0 \qquad \eta = 0$$

$$\frac{d}{d\bar{t}}\left[\bar{X}\int_0^1 \bar{\rho}_i d\eta\right] = \frac{k_i(p_i - p_{ib})L}{\rho_{i0}D_{11,0}} \qquad \eta = 1$$

$$\bar{X} = \frac{1 - \sum_{i=1}^{n-1}\rho_{i0}\hat{V}_i}{1 - \sum_{i=1}^{n-1}\rho_{i0}\hat{V}_i \int_0^1 \bar{\rho}_i d\eta} \qquad \eta = 1$$

Initial conditions

$$\bar{\rho}_i(0,\eta) = 1 \qquad \bar{X}(0) = 1 \qquad \bar{T}(0) = 1$$

Heat transfer

$$\frac{d\bar{T}}{d\bar{t}} = \frac{A + B + E - A\bar{T}}{F + \bar{X}}$$

$$A = \frac{L(h^G - h^g)}{D_{11,0}\rho^p \hat{C}_P^p} \qquad B = \frac{L\sum_{i=1}^{n-1}\Delta H_{vi}k_i(p_i - p_{ib})}{D_{11,0}\rho^p \hat{C}_P^p(T^G - T_0)}$$

$$F = \frac{\rho^s \hat{C}_P^s H}{\rho^p \hat{C}_P^p L} \qquad E = \frac{Lh^g(T^g - T^G)}{D_{11,0}\rho^p \hat{C}_P^p(T^G - T_0)}$$

$$j_i^{\neq} = \sum_{j=1}^{n-1} D_{ij}\frac{\partial \rho_j}{\partial x} = 0 \qquad x = 0 \tag{16}$$

The boundary condition at the interface of the film and gas phase is expressed using the following definition, where mass transfer in the gas phase is represented by the mass-transfer coefficient:

$$-\sum_{j=1}^{n-1} D_{ij}\frac{\partial \rho_j}{\partial x} - \rho_i\frac{dX}{dt} = k_i(p_i - p_{ib}) \qquad x = X(t) \tag{17}$$

where k_i, p_i, and p_{ib} are mass-transfer coefficient, partial pressure at the interface and partial pressure in the gas phase of component i, respectively.

The time dependence for the boundary of the gas-film interface is obtained by using the jump balance for the polymer at this interface and recognizing that no polymer is in the gas phase.

$$\frac{dX}{dt} = \left[\frac{\sum_{j=1}^{n-1} j_j^{\neq}\hat{V}_j}{\left(1 - \sum_{j=1}^{n-1}\rho_j\hat{V}_j\right)}\right] \qquad x = X(t) \tag{18}$$

The heat transfer in the polymer solution and substrate using the heat balance for the polymer phase is:

$$\frac{dT}{dt} = \frac{h^g(T - T^g) + \sum_{i=1}^{n-1}\Delta H_{vi}k_i(p_i - p_{ib}) + h^G(T - T^G)}{\rho^p \hat{C}_P^p X(t) + \rho^s \hat{C}_P^s} \tag{19}$$

Table IV lists the summary of equations for the drying model using the coordinate transformation to facilitate the numerical solution for the moving boundary of the film as follow:

$$\eta = \frac{x}{X(t)} \tag{20}$$

Kirkaldy et al.[18] showed that the Onsager consistency requires that the matrix of diffusion coefficients have real and positive eigenvalues. For a ternary system, this can be expressed as:

$$\begin{aligned} &D_{11} + D_{22} > 0 \\ &D_{11}D_{22} - D_{12}D_{21} \geq 0 \\ &(D_{11} + D_{22})^2 - (D_{11}D_{22} - D_{12}D_{21}) \geq 0 \end{aligned} \tag{21}$$

In the simulation, all four diffusion coefficients obeyed the above constraints and no material balance was violated.

RESULTS AND DISCUSSIONS

The drying model was used to predict the concentration of toluene and nitrogen in the film during the

TABLE V
Initial Data and Operating Conditions for Poly(vinyl acetate) and Toluene[17]

Initial conditions	
Initial concentration of solvent (ρ_{10})	0.64 g/cm^3
Film thickness (L)	0.0229 cm
Temperature (T_0)	296 K
Coating parameters	
Heat capacity ($\hat{C}_P^p$)	1.65 J/g K
Heat of vaporization of solvent ΔH_v	360 J/g
Substrate parameters	
Heat capacity ($\hat{C}_P^s$)	1.67 J/g K
Density (ρ^s)	1.4 g/cm^3
Thickness (H)	0.0036 cm
Operating conditions	
Base side heat transfer coefficient (h^g)	0.0036 W/cm^2 K
Coating side heat transfer coefficient (h^g)	0.0036 W/cm^2 K
Base side temperature (T^G)	349 K
Coating side temperature (T^G)	349 K
Mass transfer coefficient (k_1)	6.02×10^{-9} s/cm

drying process and whether or not there was the potential for the nitrogen to become supersaturated. Diffusion in the ternary system is described by four diffusion coefficients, where D_{11} and D_{22} are the main mutual-diffusion coefficients and D_{12} and D_{21} are the cross mutual-diffusion coefficients.

Throughout this article the initial conditions and operating conditions for the drying simulations were those presented in Table V. As a first approximation, the cross mutual-diffusion coefficients were assumed to be zero and the Zielinski and Hanely[14] approach for mutual diffusion was used. The initial concentration of nitrogen in the polymer was assumed to be at equilibrium with the initial toluene concentration and was predicted from the GCLF-EoS. Figure 7 shows relative nitrogen saturation (RNS) during the drying for different positions in the polymer film. The RNS is defined as

$$\mathrm{RNS} = \frac{[N_2(drying) - N_2(sat.)]}{N_2(sat.)} \tag{21}$$

where $N_2(drying)$ is the concentration of nitrogen during the drying and $N_2(sat.)$ is the concentration of nitrogen at its saturation. Positive values of the RNS would indicate supersaturation of nitrogen. The curves in Figure 7 are for three different positions in the film as indicated by the dimensionless thickness. $\eta = 0$ is at the substrate surface and $\eta = 1$ is the polymer-gas interface. The negative values indicate that nitrogen diffuses faster than toluene and therefore it cannot be supersaturated within the film if there are no cross-diffusion terms in the model. This case represents the ideal system in which the diffusion of one component does not affect the diffusion of others.

Figure 8 shows the nitrogen weight fraction at the position near the polymer-gas interface ($\eta = 0.94$) as

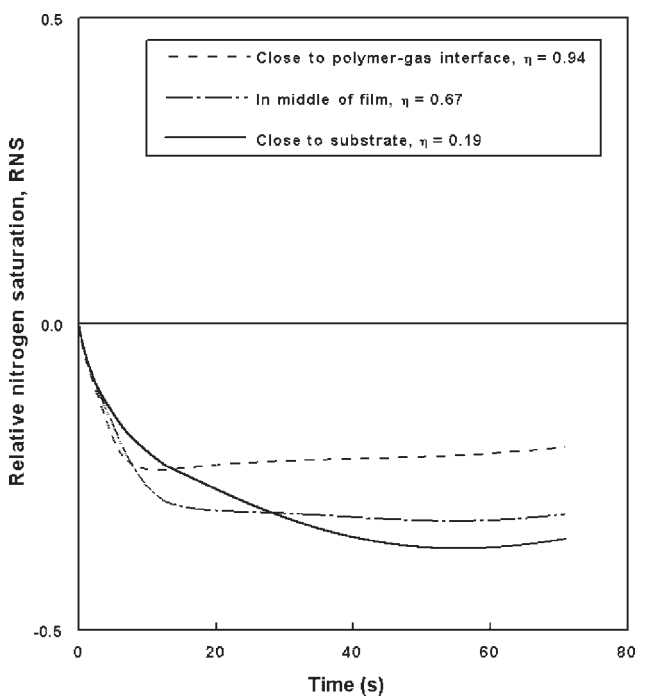

Figure 7 Relative nitrogen saturation during the drying at different positions in the PVAc-toluene-nitrogen and considering the cross mutual-diffusion coefficients, D_{12} and D_{21}, to be zero. The Zielinski and Hanley model was used for D_{11} and D_{22}.

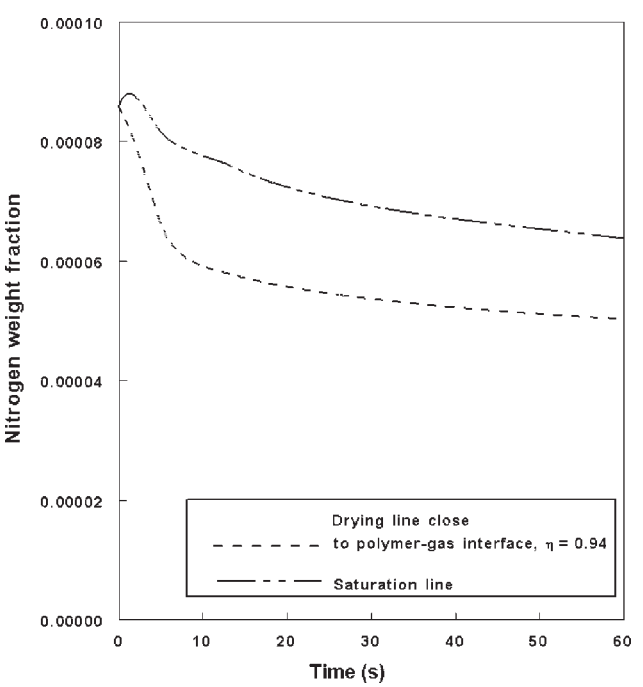

Figure 8 Saturation and drying lines for nitrogen in the system of PVAc-toluene-nitrogen during the drying process and considering the cross mutual-diffusion coefficients, D_{12} and D_{21}, to be zero. The Zielinski and Hanley model was used for D_{11} and D_{22}.

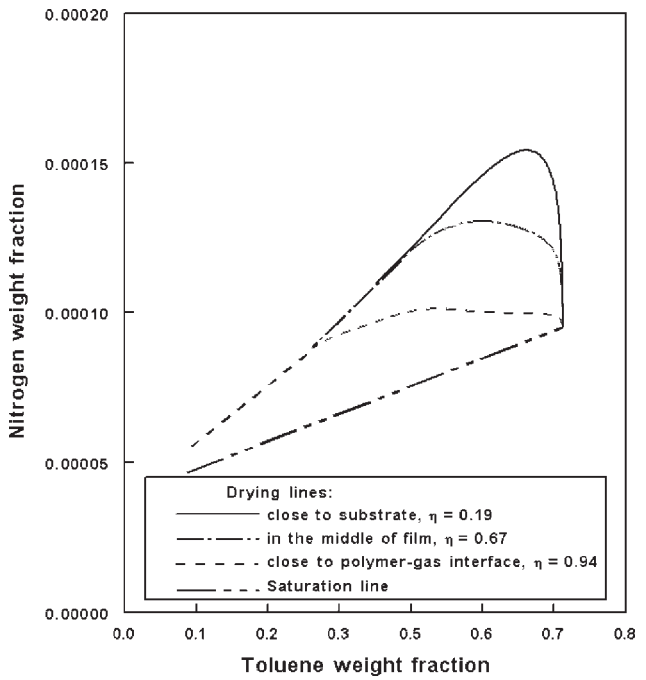

Figure 9 Saturation and drying lines for nitrogen in the system of PVAc-toluene-nitrogen during the drying process at 40°C when the mutual cross-diffusion coefficients are included.

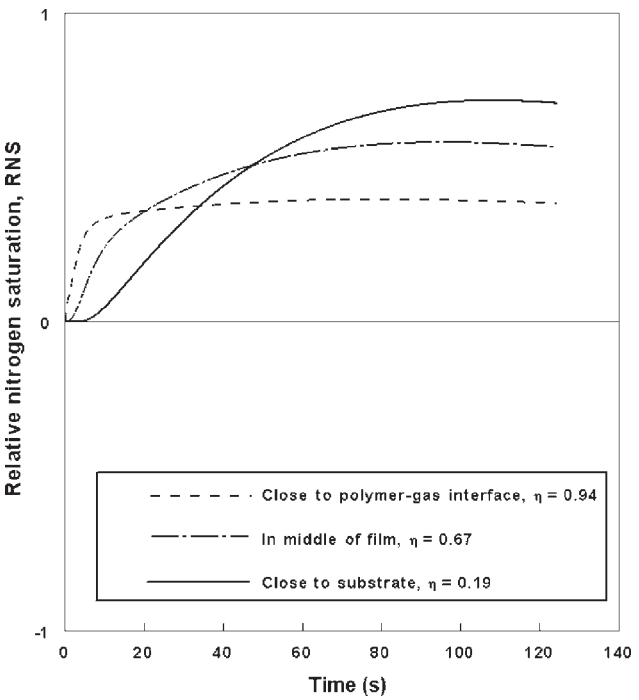

Figure 10 Relative nitrogen saturation during the isothermal drying at different positions in the film (PVAc-toluene-nitrogen) at 40°C when the cross mutual-diffusion coefficients are included.

a function of time and the predicted saturated nitrogen. The nitrogen never becomes supersaturated when the cross mutual-diffusion coefficients were neglected.

The drying model was next applied with all four diffusion coefficients and the different diffusion models to predict the nitrogen concentration within the film for isothermal drying. Figure 9 shows the saturation line and the isothermal drying line for nitrogen at 40°C using and the Price and Hadj Romdhane[15] diffusion coefficient model and Table V for initial data. This analysis predicted that the drying lines for different positions within the film are above the saturation line, and thus, nitrogen becomes supersaturated. The results confirm our bench experiment observations that bubbles can be created at temperatures well below the bubble point temperature of the solution. The results also indicate that the nitrogen concentration becomes more supersaturated at the interface of the film and substrate. Therefore, nitrogen has the potential to make bubbles from any nucleation sites at the film-substrate interface or within the film. Cavities within the film may also be caused by impurities. At early times, the nitrogen concentration (weight fraction) increases to a maximum amount due to the toluene diffusing out of the film. After nitrogen passes the maximum, all drying curves decreases with the same slope and all lines converge to a common limit. At the limit of zero concentration of toluene, nitrogen concentration decreases to its solubility in PVAc. Figure 10 shows relative nitrogen saturation (RNS) during the drying for different positions in the polymer film with cross-diffusion terms at 40°C. Again the positive value for lines indicates that nitrogen becomes

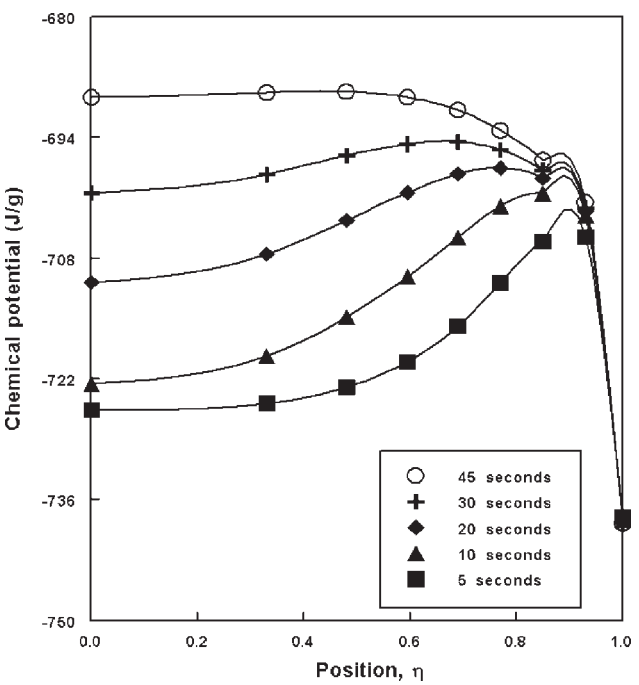

Figure 11 Chemical potential of nitrogen at different positions, η, and time intervals.

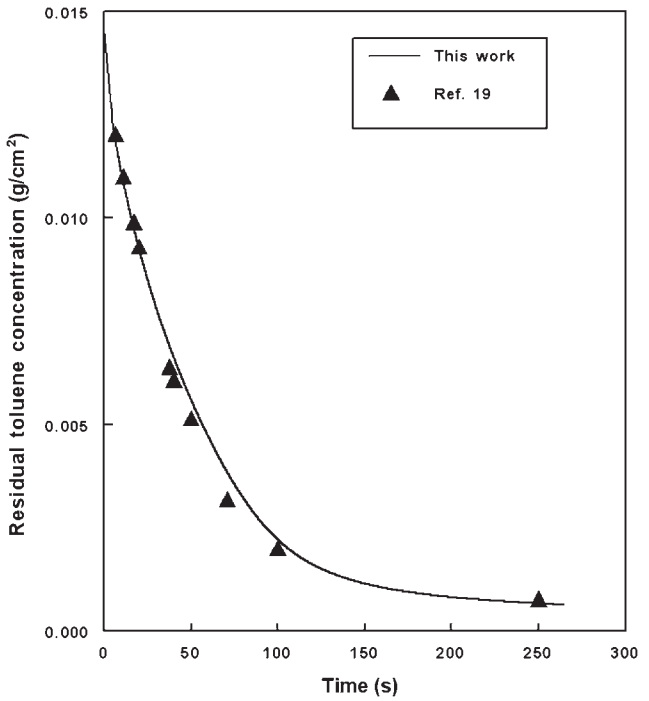

Figure 12 Comparison of the experimental[19] and predicted residual toluene concentration during the drying the PVAc-toluene system.

supersaturated within the film. As expected from Figures 4 and 5, the other models [Alsoy and Duda,[13] Zielinski and Hanley[14]] predicted the same behavior.

Figure 11 shows the chemical potential of nitrogen at different positions and times for the first 45 s. The chemical potential of nitrogen increases near the polymer-gas interface ($\eta = 1$) after 5 s. The chemical potential of nitrogen closer to the substrate ($\eta = 0$) is less than its chemical potential at the interface. Therefore, it is expected that the nitrogen transfers from the interface to the substrate and, thus, this can explain the supersaturation of nitrogen. After 45 s, the chemical potential at the substrate is greater than any places in the film and then nitrogen will move from the substrate to the interface

The drying model for the ternary system of PVAc-toluene-nitrogen was compared with the experimental data for drying the binary system of poly(vinyl acetate)-toluene[19] in the case of nonisothermal drying and again using the operating conditions listed in Table V. Figure 12 presents the experimental data along with the ternary drying model predictions for residual toluene concentration as a function of time. The Price and Hadj Romdhane model was used for the mutual-diffusion coefficients. The graph shows the drying model is in good agreement with the experimental data. Figure 13 shows the simulation for the coating temperature which is in good agreement with experimental data.

Figure 14 shows relative nitrogen saturation (RNS) during the drying of the polymer film at three different positions ($\eta = 0.16$, 0.67, and 0.94) in the polymer solution and considering cross-diffusion terms in the model. The bubble-point pressure at the maximum amount of nitrogen which is located at the

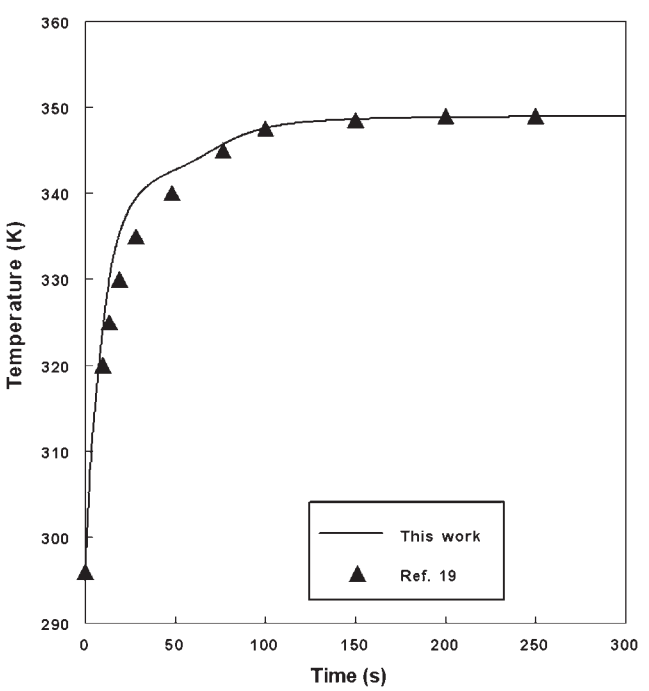

Figure 13 Comparison of the experimental[19] and predicted temperature of the coating during the drying the PVAc-toluene system.

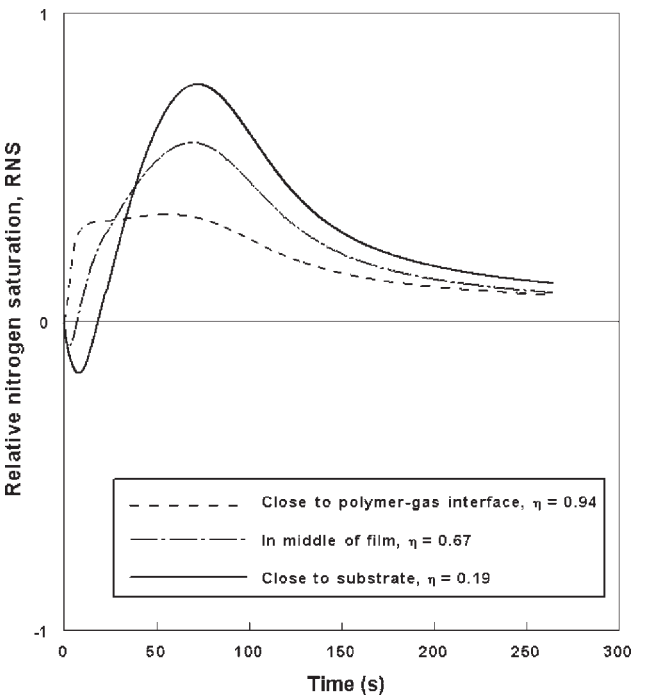

Figure 14 Relative nitrogen saturation during the nonisothermal drying at different positions in the film (PVAc-toluene-nitrogen) when the cross mutual-diffusion coefficients are included.

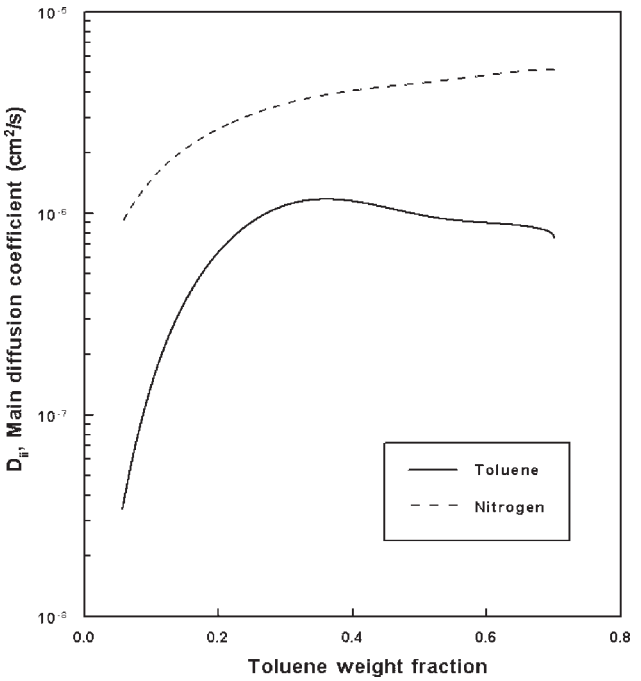

Figure 15 Main mutual-diffusion coefficients of toluene and nitrogen at $\eta = 0.94$.

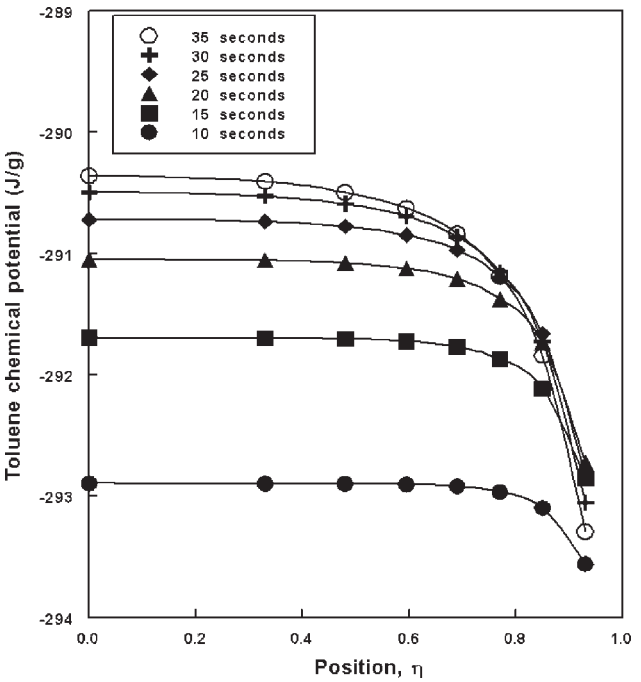

Figure 17 Chemical potential of toluene at different positions, η, and time intervals.

interface of film and substrate was found to be 25 psia. This pressure has the capability to convert any available nucleation sites to a bubble.

Figure 15 show the main diffusion coefficients for toluene and nitrogen at $\eta = 0.94$. The main diffusion coefficient of toluene is similar to its mutual-diffusion coefficient in the binary system of PVAc-toluene because the free volume of system is not affected by the small amount of nitrogen. But the main diffusion coefficient of nitrogen is larger than its mutual-diffusion coefficient in the binary system of PVAc-nitrogen by about one order of magnitude. This larger

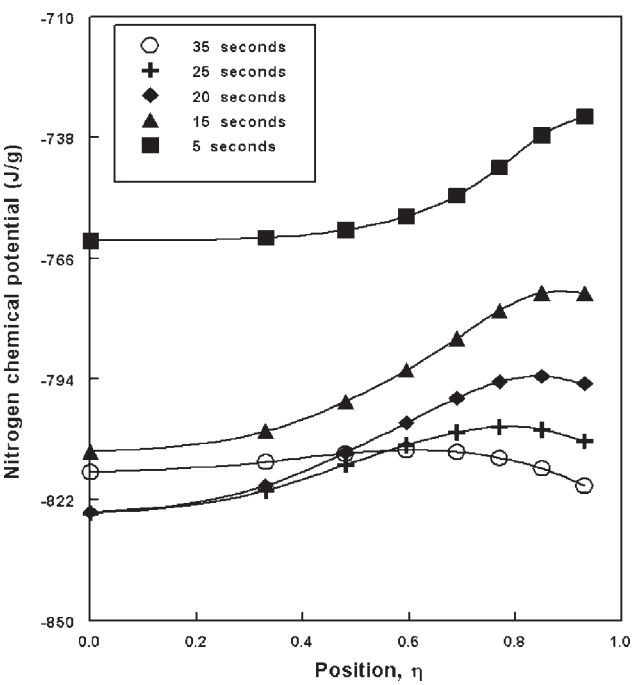

Figure 16 Chemical potential of nitrogen at different positions, η, and time intervals.

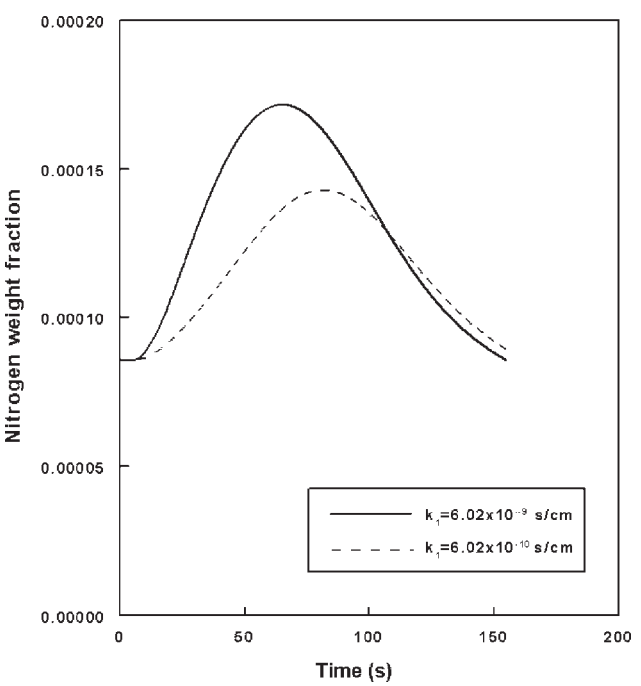

Figure 18 Effect of gas phase mass transfer coefficient, k_1, on the nitrogen content close to the substrate, $\eta = 0.19$.

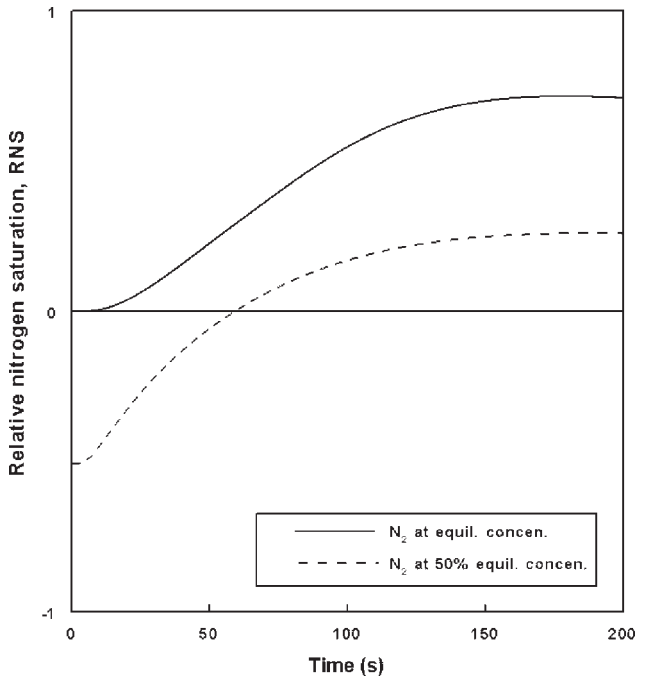

Figure 19 Comparison of relative nitrogen saturation at 50°C for two different initial concentrations of nitrogen close to the substrate, $\eta = 0.19$.

diffusivity is due to the increase in free volume with increasing toluene concentration. The main diffusion coefficient of nitrogen is larger than that for toluene in the film.

The chemical potentials of components in the mixture have important roles which affect all four mutual-diffusion coefficients. The chemical potential gradients of toluene and nitrogen in the mixture are the important factors in terms of influencing the cross-diffusion coefficients. Figures 16 and 17 show the chemical potential of nitrogen and toluene at different positions and times up to 35 s. Figure 16 shows that the chemical potential of nitrogen increases near the polymer-gas interface after 5 s. The chemical potential of nitrogen near the interface is greater than its chemical potential at the substrate. Therefore, it is expected that the nitrogen transfers from the interface area to the substrate. After 35 s, the chemical potential starts to increase near the substrate and decrease at the interface and, thus, nitrogen transfers from the substrate to the interface. Figure 17 indicates that the chemical potential of toluene near the substrate is always greater than its chemical potential at the interface and, thus, toluene always diffuses out from the film. Therefore, the increasing chemical potential of nitrogen and decreasing chemical potential of toluene in going from the substrate to the interface at the beginning of the drying can explain the supersaturation of nitrogen.

To understand the effect of gas phase mass transfer on the nitrogen supersaturation in the film, two different mass transfer coefficients were employed in the simulation. Figure 18 shows that as the mass transfer coefficient increases in the system, nitrogen becomes more supersaturated and the maximum saturation is achieved faster. This behavior supports our experimental observations that increased air flow increased bubble formation.

Our observations also indicated that the degassing of the polymer solution before drying can reduce bubble formation. To examine the effect of degassing in the simulation, nitrogen concentration was reduced to 50% of its concentration at equilibrium. Figure 19 compares the supersaturation behavior of nitrogen at 50°C at the two different initial nitrogen concentrations. The graph indicates that reducing the nitrogen concentration by 50% will decrease the supersaturation, but it can not completely eliminate it. This means that degassing the polymer solution can reduce bubble formation as expected if the nitrogen is the causation of the bubbles.

SUMMARY AND CONCLUSION

The multicomponent drying model based on the volume-average velocity was used for the system of PVAc-toluene-nitrogen. The drying model has been verified to be in good agreement with experimental data for the binary system of PVAc- nitrogen. For a ternary system, the drying model was capable of predicting nitrogen and toluene concentrations as a function of time in the film.

Supersaturation of nitrogen in the film was identified as the mechanism for the formation of bubble defects during the drying process. The cross-diffusion terms in the mass transfer model were essential for the development of nitrogen supersaturation.

The results from the prediction indicate that:

1. Nitrogen becomes supersaturated even below the bubble-point temperature of solution.
2. Nitrogen becomes more supersaturated at higher temperatures.
3. Degassing the system delays the onset and extent of supersaturation.
4. Reducing the mass-transfer resistance in the gas phase leads to more pronounced supersaturation.
5. The key to supersaturation is the chemical potential of nitrogen within the film.
6. The different diffusion models lead to qualitatively similar predictions for the supersaturation of nitrogen.

The simulation results supported all our experimental observations regarding bubble formation.

This effect would be exhibit by all polymer-solvent system in which the nitrogen is more soluble in the solvent than in the polymer. In such systems the cross-diffusion coefficient will play a dominant role.

NOMENCLATURE

$\hat{C}_P$	heat capacity of (J/g K)
D_{ii}	main diffusion coefficients
D_{ij}	cross-diffusion coefficients
D_{0i}	pre-exponential factor of component i (cm^2/s)
$D_{11,0}$	reference diffusivity of component 1 at initial composition and temperature in the polymer phase (cm^2/s)
E	energy required to overcome attractive forces from neighboring molecules (cal/mol)
H	substrate thickness (cm)
h^G	heat transfer coefficient of the gas phase on top of the polymer solution (W/cm^2 K)
h^g	heat transfer coefficient of the gas phase below the substrate (W/cm^2 K)
$j_i^{\neq}$	mass diffusive flux of component of i with respect to volume-average velocity (g/cm^2 s)
K_{1i}/γ	free volume parameter of component i (cm^3/g K)
K_{2i}	free volume parameter of component i (K)
k_i	mass-transfer coefficient of component i in the gas phase (s/cm)
L	initial thickness of the polymer solution (cm)
M_i	molecular weight.
p_i	partial pressure of component i in the gas phase (bar)
p_{ib}	bulk gas partial pressure of component i in the gas phase (bar)
R	gas constant (cal/mol K)
T	temperature (K)
T_{gi}	glass transition temperature of component i (K)
T^G	temperature of the gas phase on top of the polymer solution (K)
T^g	temperature of the gas phase below the substrate (K)
$\hat{V}_i^*$	specific critical hole free volume (cm^3/g)
$\hat{V}_i$	partial specific volume of component i (cm^3/g)
v_i	species velocity of component i in the mixture.
ω_i	weight fraction of component i
$X(t)$	thickness of the polymer solution at time t (cm)
ΔH_{vi}	heat of vaporization of component i (J/g)
μ_i	chemical potential of component i
ρ_i	mass density of component i in the system
ρ_{io}	initial mass density of component i in the system
ρ^s	substrate density (g/cm^3)
ζ_{ij}	frictional force between molecules i and j
ξ_{ij}	ratio of i and j jumping units

Subscripts

P	polymer
S	substrate
1	toluene
2	nitrogen
3	poly(vinyl acetate)

References

1. Pourdarvish, R.; Danner, R. P.; Duda, J. L. J Appl Polym Sci 2008, 108, 1407.
2. Lee, B.-C.; Danner, R. P. AIChE J 1996, 42, 837.
3. Vrentas, J. S.; Duda, J. L. J Polym Sci Part B: Polym Phys 1977, 15, 403.
4. Vrentas, J. S.; Duda, J. L. J Polym Sci Part B: Polym Phys 1977, 15, 417.
5. Vrentas, J. S.; Duda, J. L.; Ling, H. C. J Polym Sci Part B: Polym Phys 1984, 22, 459.
6. Zielinski, J. M.; Duda, J. L. AIChE J 1992, 38, 405.
7. Vrentas, J. S.; Duda, J. L.; Ling, H. C.; Hou, A. C. J. Polym Sci Part B: Polym Phys 1985, 23, 289.
8. Sugden, S. J Chem Soc 1927, 1780.
9. Bearman, R. J. J Phys Chem 1961, 65.
10. Onsager, L. Phys Rev 1931, 37, 405.
11. Onsager, L. Phys Rev 1931, 38, 2265.
12. Cussler, E. L.; Multicomponent Diffusion; Elsevier: Amsterdam, 1976.
13. Alsoy, S.; Duda, J. L. AIChE J 1999, 45, 896.
14. Zielinski, J. M.; Hanley, B. F. AIChE J 1999, 45, 1.
15. Price, P. E.; Hadj Romdhane, I. AIChE J 2003, 49, 309.
16. Vrentas, J. S.; Vrentas, C. M. J Polym Sci Part B: Polym Phys 1994, 32, 187.
17. Kirkaldy, J. S.; Zia-Ul-Haq; Weichert, D. Canad. J Phys 1963, 41, 2166.
18. Alsoy, S. Ph.D. Thesis, Department of Chem Engineering; The Pennsylvania State University, Pennsylvania, 1998.
19. Vrentas, J. S.; Duda, J. L.; Ling, H. C. J Appl Polym Sci 1985, 30, 4499.